

STRUCTURAL INVESTIGATION OF ELECTROCHEMICALLY ETCHED SILICON

B.J. HEUSER,¹ S. SPOONER,^{2,†} C.J. GLINKA,³ D.L. GILLIAM,⁴ N.A. WINSLOW⁵ and M.S. BOLEY⁵

¹University of Missouri Research Reactor Center, Columbia, MO 65211

^{2,†}Solid State Division, Oak Ridge National Laboratory, Oak Ridge, TN 37831

³Reactor Radiation Division, National Institute of Standards and Technology, Gaithersburg, MD 20899

⁴Department of Physics, Lincoln University, Jefferson City, MO 65101

⁵Department of Physics and Astronomy, University of Missouri, Columbia, MO 65211

ABSTRACT

Small-angle neutron scattering (SANS) measurements of four electrochemically etched, porous silicon (PS) samples have been performed over a wide wavevector transfer (Q) range. The intermediate to high Q results can be modeled with a non-particulate, random phase model. Correlation length scales on the order of 1 to 2 nm thought to characterize the PS skeleton have been deduced from the SANS data. The microstructural anisotropy was studied by tilting two of the samples with respect to the neutron beam. These samples exhibited an asymmetric scattering pattern at intermediate Q ($0.1 \leq Q \leq 0.6 \text{ nm}^{-1}$) in this condition. Photoluminescence spectra from all four samples have been recorded as well. A correlation appears to exist between the SANS and photoluminescence measurements. An x-ray diffraction measurement of one sample demonstrates that the PS layer retains the silicon lattice structure. Significant peak broadening is observed and is interpreted as a quasi-particle size effect. The PS particle size calculated from the x-ray diffraction measurement is equal to the correlation length obtained in the SANS measurement.

INTRODUCTION

The discovery of a form of Si with a photoluminescence efficiency much higher than that of bulk Si has led to a flurry of research activity. This unusual form of Si is created during electrochemical etching of oriented single crystal Si in hydrofluoric acid under a variety of conditions. The resultant material is very porous and often appears red in color. Electrical, photoluminescence, and structural properties of electrochemically etched, porous silicon (PS) have been extensively investigated in the past few years. Two suggested explanations for the dramatic increase in photoluminescence efficiency involve a) the quantum confinement of charge carriers in very small structures (on the order of a nanometer) created during etching [1] or b) the contamination of internal surfaces by foreign elements such as hydrogen and oxygen [2]. Complete understanding of the PS photoluminescence behavior will require accurate structural information. To this end, the goal of the work presented here was to determine bulk structural parameters characteristic of the PS material investigated.

Four PS samples were characterized with small-angle neutron scattering (SANS), two over a wide wavevector transfer range. Microstructural anisotropy and vertical uniformity for selected samples were investigated as part of this study. Photoluminescence spectra also were obtained for each sample, and a correlation between SANS behavior and photoluminescence appears to exist for our sample set. An x-ray diffraction measurement of one sample has been performed as well, with significant peak broadening evident.

EXPERIMENTAL

The PS samples were prepared first by establishing an electrical contact on p-type, boron doped (100) oriented Si. Electrochemical etching then was performed in dilute hydrofluoric acid at room temperature using a Pt cathode. Material preparation parameters are listed in Table I. No effort was made to prevent oxidation of the PS material. The samples typically spent several weeks in air at room temperature prior to all measurements.

The M1 sample consisted of five identically prepared wafers stacked together for SANS investigation; all other samples were single wafers. An important physical characteristic of the

Government under contract No. DE-AC05-84OR21400. Accordingly, the U.S. Government retains a nonexclusive, royalty-free license to publish or reproduce the published form of this contribution, or allow others to do so, for U.S. Government purposes.

MASTER

HEUSER
DISTRIBUTION OF THIS DOCUMENT IS UNLIMITED

M1 sample deserves discussion. The top layer of this particular sample material was weakly bound to the underlying PS layer. It was evident from visual inspection with a microscope that this layer had cracked and partially peeled off the underlying material. Other researchers have attributed this effect to post-etching, evaporation-induced stresses [3]. The SANS response of the M1 sample was recorded with ("before removal") and without ("after removal") this weakly bound top layer. A check of the vertical uniformity (uniformity in the direction of etching) of the M1 type PS layer was obtained with this procedure.

Table I. Sample preparation parameters.

Sample ID	Resistivity [$\Omega\cdot\text{cm}$]	% HF	HF diluted with	Current density [mA/cm^2]	Color
M1	20	12.5	87.5% H ₂ O	7 to 10	red-brown
G1	5	25	25% H ₂ O, 50% ethanol	30 to 60	red
G2	5	25	25% H ₂ O, 50% ethanol	30 to 60	red-brown
G3	5	25	25% H ₂ O, 50% ethanol	30 to 60	orange

Structural defects will coherently scatter neutrons at small angles with the approximate relationship $\ell \sim 2\pi/Q$ holding between the length scale, ℓ , of the defect and Q . The neutron wavevector transfer is defined as $Q=(4\pi/\lambda)\sin\theta$, where λ is the neutron wavelength and θ is half the scattering angle. Thus, large structural defects scatter neutrons at smaller angles, while the opposite is true at higher angles.

The neutron scattering measurements reported here were performed on the 30 meter small-angle neutron spectrometer at Oak Ridge National Laboratory (ORNL), Oak Ridge, Tennessee and on the 8 and 30 meter spectrometers at the National Institute of Standards and Technology (NIST), Gaithersburg, Maryland. An investigation of microstructural anisotropy was performed by tilting M1 and G2 with respect to the 8 meter incident neutron beam and by tilting M1 with respect to the 30 meter incident beam. All other measurements were performed with the incident neutron beam perpendicular to the PS surface. Except for the measurements where an asymmetric response was evident, all data were radially averaged.

The photoluminescence and x-ray diffraction measurements were performed at the University of Missouri Department of Physics and Astronomy at Columbia, Missouri. Photoluminescence was recorded at 300 K using a 0.85 m focal length double-grating Spex Model 1401 spectrometer equipped with a thermoelectrically cooled GaAs. Luminescence was excited in vacuum with the 488 nm line of a 5 W argon ion laser using a power of 40 mW incident on a spot size of 100 μm . The x-ray diffraction measurements were performed with a graphite monochromator and Cu K α radiation ($\lambda=1.54 \text{ \AA}$).

RESULTS AND DISCUSSION

The SANS responses of the four PS samples are shown in Fig. 1. Time constraints limited the measured range of scattering angles for the G1 and G3 samples. The SANS data are modeled with a non-particulate, random phase model [4] over the intermediate to high Q range. The functional form of this scattering behavior is given by,

$$\frac{d\Sigma}{d\Omega}(Q, L) = 8\pi\langle\eta^2\rangle \frac{L^3}{(1+Q^2L^2)^2}, \quad (1)$$

where L is the correlation length scale of the random structures within the scattering system and $\langle\eta^2\rangle$ is the mean square scattering length density fluctuation averaged over all points within the scattering system. The low Q responses of M1 and G2 are fit with a power law behavior $d\Sigma/d\Omega \sim Q^{-4}$. The parameters obtained from fitting the data in Fig. 1 are presented in Table II.

The M1 "before removal", G1, G2, and G3 intermediate to high Q data are fit reasonably well with the Debye-Bueche model. This suggests that a) the silicon-void interfaces in the PS samples investigated are sharp and smooth (i.e., discontinuous and non-fractal like [5]) and b) they randomly occupy PS sample volume. Notice that a systematic difference in the

HEOVER

2

6

DISCLAIMER

This report was prepared as an account of work sponsored by an agency of the United States Government. Neither the United States Government nor any agency thereof, nor any of their employees, makes any warranty, express or implied, or assumes any legal liability or responsibility for the accuracy, completeness, or usefulness of any information, apparatus, product, or process disclosed, or represents that its use would not infringe privately owned rights. Reference herein to any specific commercial product, process, or service by trade name, trademark, manufacturer, or otherwise does not necessarily constitute or imply its endorsement, recommendation, or favoring by the United States Government or any agency thereof. The views and opinions of authors expressed herein do not necessarily state or reflect those of the United States Government or any agency thereof.

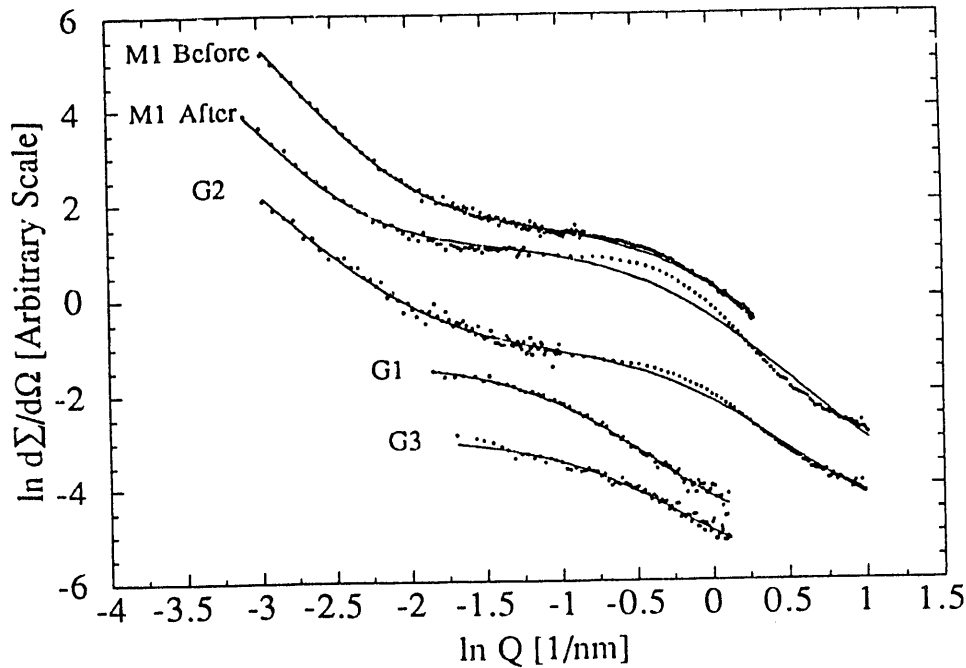


Fig. 1 SANS response of PS samples. Solid lines represent best fit of data with Eq. (1) and a power law. Individual data sets have been separated for clarity.

Table II. Random phase correlation length scales and power law exponents for PS samples.

Sample ID	L [nm]	Power law exponent n
M1 before removal	1.0	-3.5 ± 0.1
M1 after removal	1.1	-3.3 ± 0.2
G1	2.2	---
G2	0.9	-2.8 ± 0.1
G3	1.7	---

* Before and after removal refers to removal of weakly bound PS top layer.

correlation length parameter L exists between the red-brown samples (M1 and G2) and the other two samples. This point is discussed below when the photoluminescence measurements of the four PS samples are presented.

Based on the Debye-Bueche scattering behavior, average chord lengths for the two random phases can be defined as $\langle \ell \rangle_{Si} = L/\phi$ and $\langle \ell \rangle_V = L/(1-\phi)$, where the subscripts Si and V refer to the Si skeleton and void, respectively, and ϕ is the porosity. It was only possible to measure the porosity of the M1 and G2 samples, and both had porosity values of approximately 90%. The corresponding Si and void chord lengths are $\langle \ell \rangle_{Si} = 1.1, 0.8$ nm and $\langle \ell \rangle_V = 10, 7$ nm for M1 for G2, respectively. L therefore represents the correlation length of the Si skeleton when the porosity of the PS is high. As the porosity decreases, the Si chord length will increase. We therefore infer from the larger L values that the G1 and G3 samples have lower porosity values than M1 and G2.

An interference effect seems to be present in the samples measured over an extended Q range. This is visible as a shoulder at intermediate Q in the M1 "after removal" and G2 sample data. (The absence of this effect in the G1 and G3 data may be an artifact of the limited measurement range.) Similar shouldering in PS has been observed in small-angle x-ray scattering measurements performed by Vezin et al. [6]. These authors interpreted this as an interference between scattering centers that make up the PS material. The spacing and size of the PS scattering centers must be somewhat irregular given the very broad, shoulder-type behavior observed.

HEWNER

The structure of the PS material, at least that of the M1 material, does not appear to be vertically uniform. In general, the two M1 curves shown in Fig. 1 are similar; the correlation lengths and power law exponents are equal to within experimental error. However, the value of L for the M1 "after removal" sample is uncertain based on the fit of Eq. (1) to the data over the intermediate to high Q range. Furthermore, the plateau and interference shoulder are more pronounced in the M1 "after removal" curve. This is attributed to a lower value of porosity for the underlying PS material. This statement is based in part on the work of Vezin et al., which demonstrates the effect that porosity has on the small-angle scattering behavior of PS [6]. These authors observed a degradation in the interference effect as the PS porosity increased. The fact that the underlying PS material has a lower porosity is not surprising: The upper portions of silicon are exposed to the electrochemical etching process for longer times and become more porous.

The low Q behavior observed for the M1 and G2 samples is consistent with large defects present in the PS material. The size of the defects must extend beyond 100 nm because the low Q power law behavior extends below $Q \sim 0.05 \text{ nm}^{-1}$. The low Q power law exponent of the M1 sample before and after removal of the top layer is equal within statistical error, indicating that the structural form of these extended defects is vertically uniform.

The possibility of microstructural anisotropy in the M1 (top layer removed) and G2 sample materials was also investigated by SANS. Fig. 2 demonstrates the effect of tilting the M1 sample 20° about an axis perpendicular to the floor. The G2 data showed little difference from the intermediate Q M1 measurement and are not shown. The horizontal and vertical sector averages in this figure are averages over pie-shaped areas on the detector deviating $\pm 15^\circ$ from the horizontal and vertical detector center-lines, respectively. The no-tilt M1 measurement, omitted for clarity, bisects the vertical and horizontal sector average curves more or less equally. Based on Fig. 2, a certain degree of structural anisotropy does exist in this PS sample that extends over length scales of approximately 10 to 60 nm. It is interesting to note the microstructural anisotropy disappears beyond length scales of approximately 60 nm.

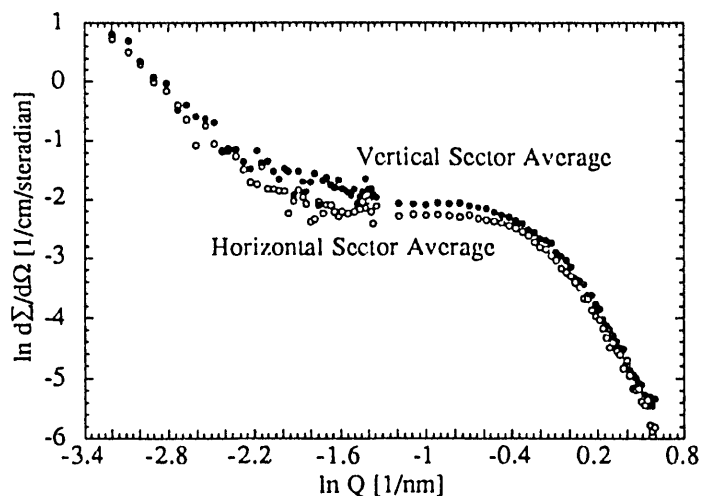


Fig. 2 Effect of tilting M1 sample (after removal of top layer) 20 degrees about a vertical axis. Microstructural anisotropy is evident over length scales from 10 to 60 nm.

The photoluminescence spectra for all samples are shown in Fig. 3. The asymmetric peak shapes from the M1 and G2 samples are due, at least in part, to the detection system efficiency going to zero at 930 nm. Notice the marked similarity between the M1 and G2 spectra, and the dissimilarity between these two spectra and those obtained from G1 and G3. The M1 and G2 measurements are characterized by significant structure in the peak region. Similar structure has been observed in PS photoluminescence spectra by other researchers and attributed to high porosity [7]. This interpretation is consistent with the porosity measurements of M1 and G2. Correlations may exist between SANS determined structural characteristics and photoluminescence behavior: The two samples with irregular photoluminescence spectra have systematically lower correlation length scales. In addition, this interrelationship seems to depend on the color of the PS.

The x-ray diffraction measurement of M1 type PS is shown in Fig. 4. The two curves are measurements of a bulk Si standard sample and M1 type PS material that was removed from the Si substrate (PS material was scraped off the Si substrate using a small spatula). Both samples were measured in a quartz capillary at room temperature. Significant peak broadening is evident

HEUER

Y
6

in the PS measurement that we interpret as a quasi-particle size effect ("quasi" because we believe these are very small, *non-particulate* regions of Si). An approximate particle size can be calculated using the Scherrer equation [8], $N = \lambda / (\Delta 2\theta a(hkl) \cos\theta)$ where N is the number of unit cells that make up the particle, $\Delta 2\theta$ is the diffraction peak width, $a(hkl)$ is the (hkl) interplanar spacing, and θ is the Bragg angle. The particle size diameters calculated from the (111), (220), and (311) peak widths are all consistent and equal to approximately 1 nm. This value is also consistent with the $\langle \ell \rangle_S$ chord length obtained from the M1 SANS measurement.

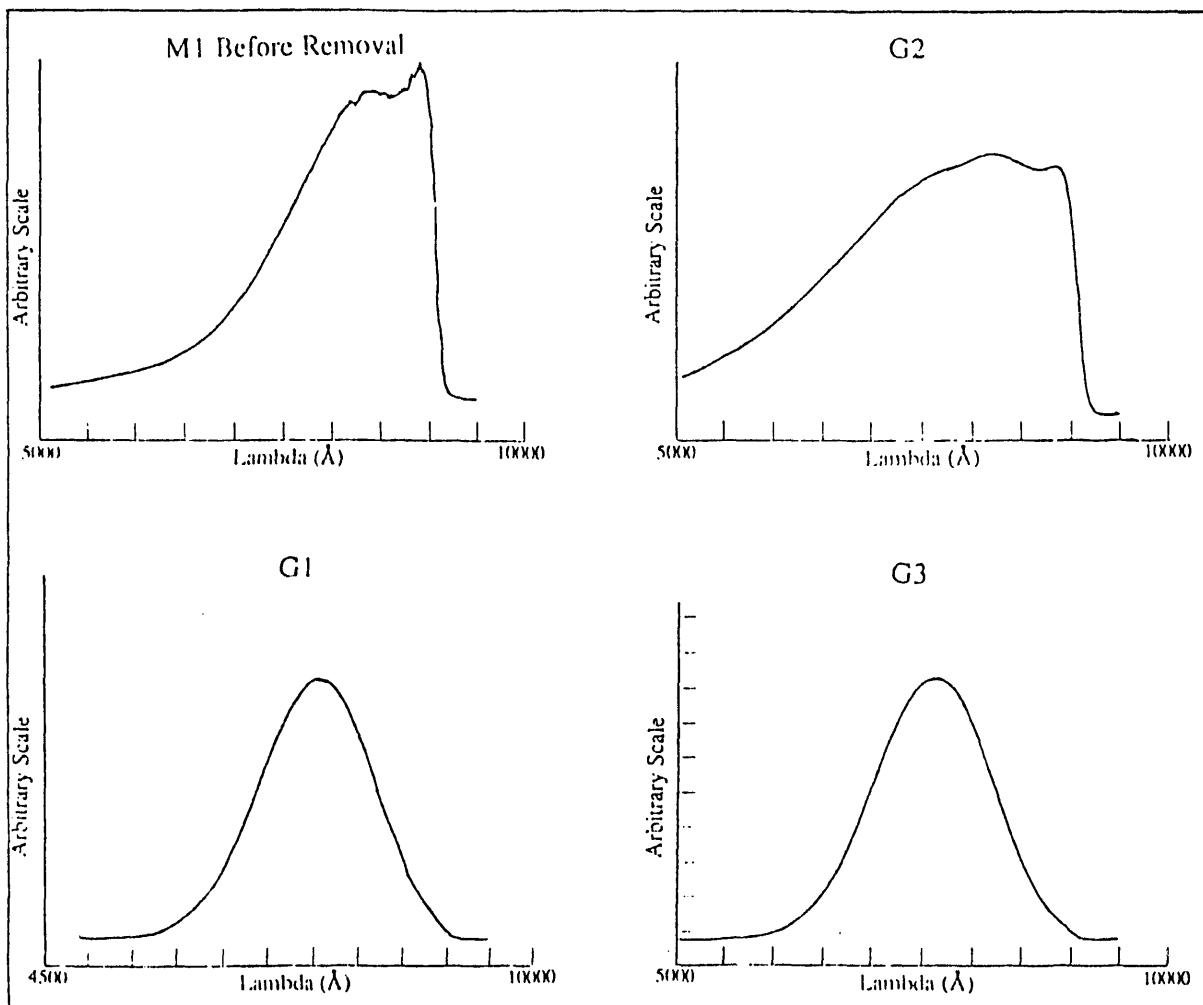


Fig. 3 Photoluminescence spectra for the four PS samples.

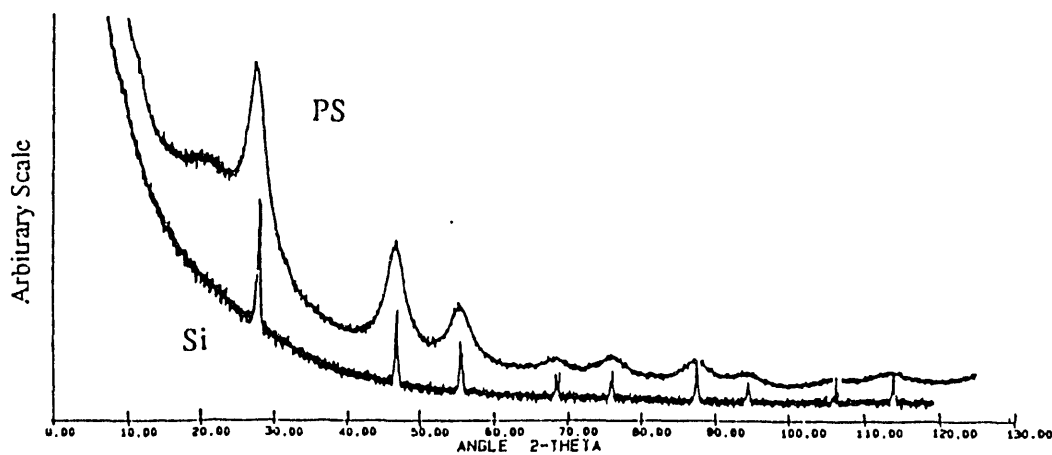


Fig. 4 X-ray diffraction measurement of M1 type PS material.

HEUGER

An additional diffraction peak is visible below (smaller diffraction angle) the (111) peak in Fig. 4. This broad peak, which has $2\pi/Q$ value 0.45 nm, cannot be associated with bulk Si lattice structure. It may be the result of oxidation of the internal PS surfaces. New measurements are being planned to further investigate this behavior.

CONCLUSIONS

1. The structural characteristics of four PS samples have been investigated with SANS. The intermediate to high Q data can be represented with a non-particulate, random phase model, indicating that the Si skeleton-void interfaces are random and discontinuous. Correlation length scales on the order of 1 to 2 nm are deduced from the SANS measurements. A low Q power law behavior was observed in the M1 and G2 SANS measurements. This behavior is the result of large (≥ 100 nm), isotropic defects in the PS layer.

2. The photoluminescence measurements of the four samples may show the effect of porosity, with the high porosity PS layers (M1 and G2 samples) exhibiting irregular structure in the peak region. In addition, systematic differences in the correlation length scales exist for our sample set that may depend on the sample photoluminescence behavior. Specifically, the two samples with more typical photoluminescence spectra (G1 and G3) are characterized by correlation lengths approximately a factor of two greater than the samples with irregular photoluminescence spectra.

3. Vertical uniformity and microstructural anisotropy were investigated as well. The SANS response of the M1 sample was found to depend on the depth of the PS layer. The effect of microstructural anisotropy was observed in measurements with the M1 and G2 samples tilted with respect to the SANS beam. This anisotropy extends over length scales of approximately 10 to 60 nm, disappearing at greater length scales.

4. The M1 type PS material was found to retain the bulk Si lattice structure in an x-ray powder diffraction measurement. Significant peak broadening was observed in this measurement that is interpreted as a quasi-particle size effect. The particle size deduced from the peak broadening is approximately 1 nm. This is equal to the average chord length thought to characterize the M1 sample Si skeleton deduced from the SANS measurements.

ACKNOWLEDGMENT

The authors are grateful to Drs. V. Petrova-Koch (Technische Universitat Munchen, Germany) and A. Yelon (Ecole Polytechnique, Montreal, Canada) for supplying some of the porous Si samples used in this work. The authors also thank Dr. G. Wignall (ORNL) for his help with the SANS measurements performed at Oak Ridge. BJH is very grateful to Drs. P. Pfeifer and F. Ross (University of Missouri) for illuminating discussions concerning the SANS data and for help with the x-ray diffraction measurements. This material is based upon activities supported by the National Science Foundation under Agreement No. DMR-9122444.

REFERENCES

- † Managed by Martin Marietta Energy Systems, Incorporated under Contract DE-AC05-84OR21400 for the U.S. Department of Energy.
- 1) L.T. Canham, Appl. Phys. Lett. **57**, 1046 (1990).
 - 2) C. Tsai, K.-H. Li, J. Sarathy, S. Shih, J.C. Campbell, B.K. Hance, and J.M. Whit, Appl. Phys. Lett. **59**, 2814 (1991).
 - 3) L.E. Friedersdorf, P.C. Searson, S.M. Prokes, O.J. Glembocki, and J.M. Macauley, Appl. Phys. Lett. **60**, 2285 (1992).
 - 4) P. Debye and A.M. Bueche, J. Appl. Phys. **20**, 518 (1949).
 - 5) In the limit of high Q, the Debye-Bueche law evolves to a $1/Q^4$ behavior typical of sharp, smooth interfaces. Surfaces exhibiting fractal dimensionality, on the other hand, obey a $1/Q^3$ to $1/Q^4$ law. For a derivation of the fractal small-angle scattering law, see P.W. Schmidt, J. Appl. Cryst. **24**, 414 (1991).
 - 6) V. Vezin, P. Goudeau, A. Naudon, A. Halimaoui, and G. Bomchil, Appl. Phys. Lett. **60**, 2625 (1992).
 - 7) B. Hamilton, Bull. Am. Phys. Soc. **37**, 669 (1992).
 - 8) L.H. Schwartz and J.B. Cohen, Diffraction From Materials (Academic Press, New York, 1977), p. 379.

HENDER

6
6

**DATE
FILMED**

8 / 17 / 93

END

